Supporting information for

Field characterization of the $PM_{2.5}$ Aerosol Chemical Speciation Monitor: insights into the composition, sources and processes of fine particles in Eastern China

Yunjiang Zhang[1-4], Lili Tang[1,2], Philip L. Croteau[5], Olivier Favez[3], Yele Sun[6], Manjula R. Canagaratna[5], Zhuang Wang[1], Florian Couvidat[3], Alexandre Albinet[3], Hongliang Zhang[7], Jean Sciare[8], André S. H. Prévôt[9], John T. Jayne[5], Douglas R. Worsnop[5]

[1]Jiangsu Collaborative Innovation Center of Atmospheric Environment and Equipment Technology, Nanjing University of Information Science and Technology, Nanjing 210044, China

[2]Jiangsu Environmental Monitoring Center, Nanjing 210036, China

[3]Institut National de l'Environnement Industriel et des Risques, Verneuil-en-Halatte, 60550, France

[4]Laboratoire des Sciences du Climat et de l'Environnement, CNRS-CEA-UVSQ, Université Paris-Saclay, Gif sur Yvette, 91191, France

[5]Aerodyne Research, Inc., Billerica, Massachusetts 01821, United States

[6]State Key Laboratory of Atmospheric Boundary Layer Physics and Atmospheric Chemistry, Institute of Atmospheric Physics, Chinese Academy of Sciences, Beijing 100029, China

[7]Nanjing Handa Environmental Science and Technology Limited, Nanjing 211102, China

[8]The Cyprus Institute, Environment Energy and Water Research Center, Nicosia, Cyprus

[9]Laboratory of Atmospheric Chemistry, Paul Scherrer Institute, Villigen PSI 5232, Switzerland

Correspondence to: L. L. Tang (lily3258@163.com) and Y. L. Sun (sunyele@mail.iap.ac.cn)

Pages 9

Figures 13

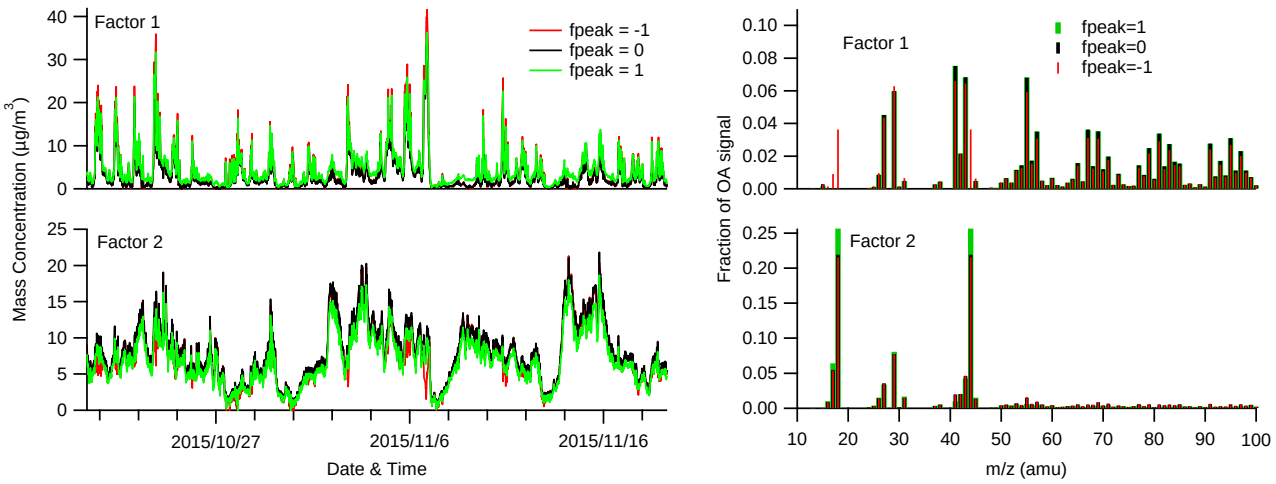

Figure S1. Time series and mass spectral profiles of 2-factor PMF solution of the PM_1 ACSM dataset at three different fpeak values.

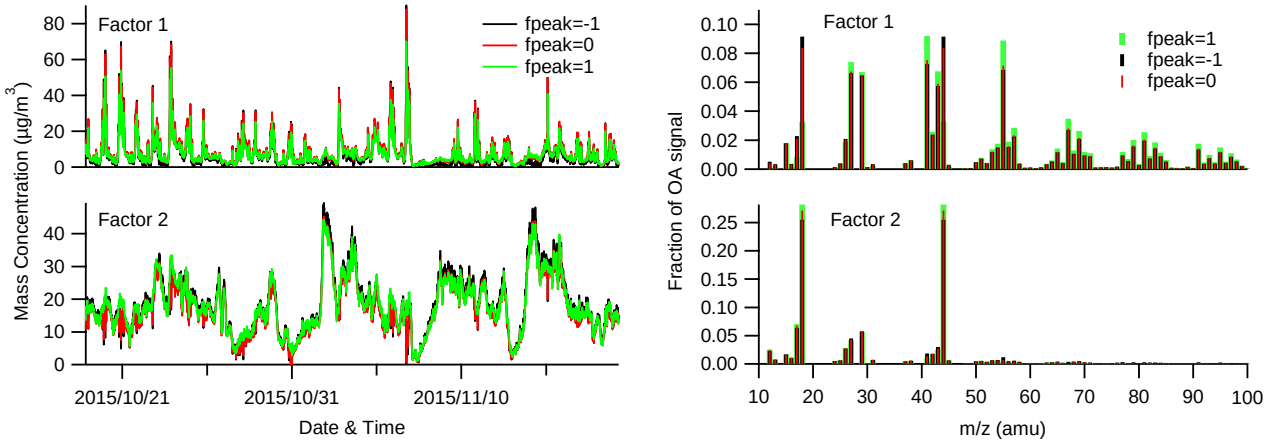

Figure S2. Time series and mass spectral profiles of 2-factor PMF solution of the $PM_{2.5}$ ACSM dataset at three different fpeak values.

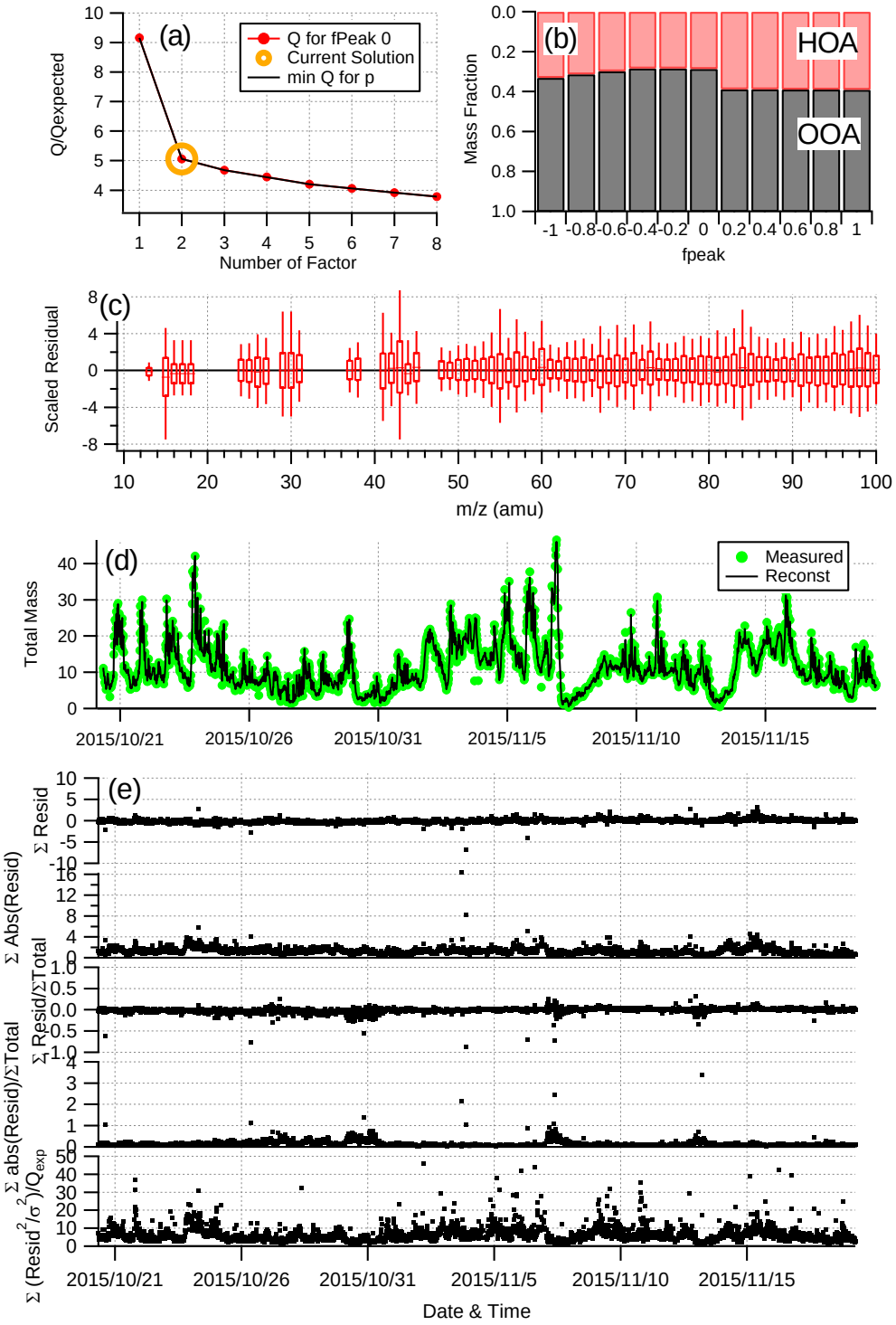

Figure S3. Summary of key diagnostic plots of the PM_1-ACSM PMF results for 2-factor solution: (a) Q/Q_{exp} as a function of number of factors, (b) mass fraction of OOA and HOA as a function of FPEAK, (c) the box and whiskers plot showing the distributions of scaled residuals for each m/z, (d) a comparison of the measured mass with the PMF reconstructed mass, (e) time series of the residual diagnostics and Q/Q_{exp} for each point in time.

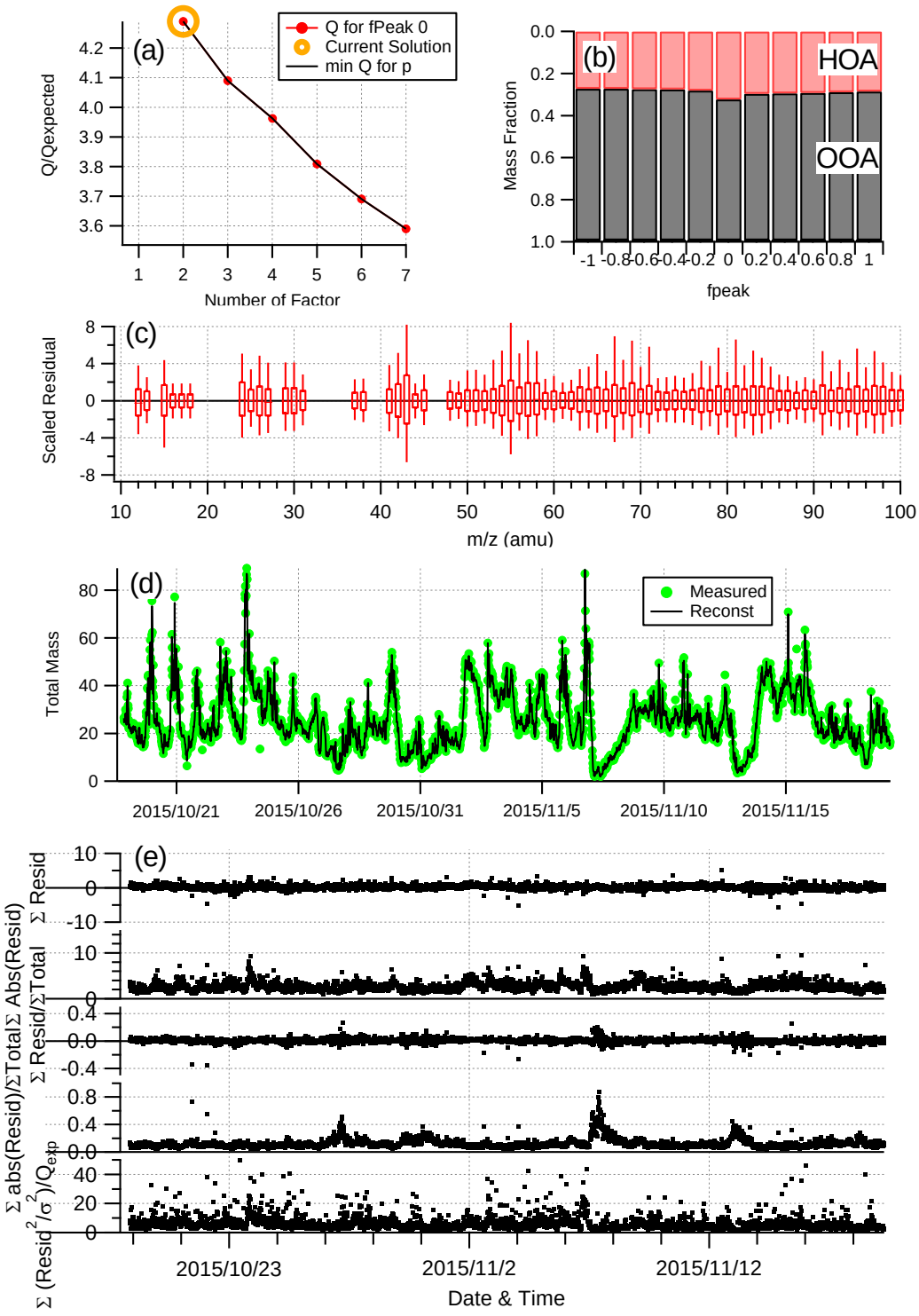

Figure S4. Summary of key diagnostic plots of the $PM_{2.5}$-ACSM PMF results for 2-factor solution: (a) Q/Q_{exp} as a function of number of factors, (b) mass fraction of OOA and HOA as a function of FPEAK, (c) the box and whiskers plot showing the distributions of scaled residuals for each m/z, (d) a comparison of the measured mass with the PMF reconstructed mass, (e) time series of the residual diagnostics and Q/Q_{exp} for each point in time.

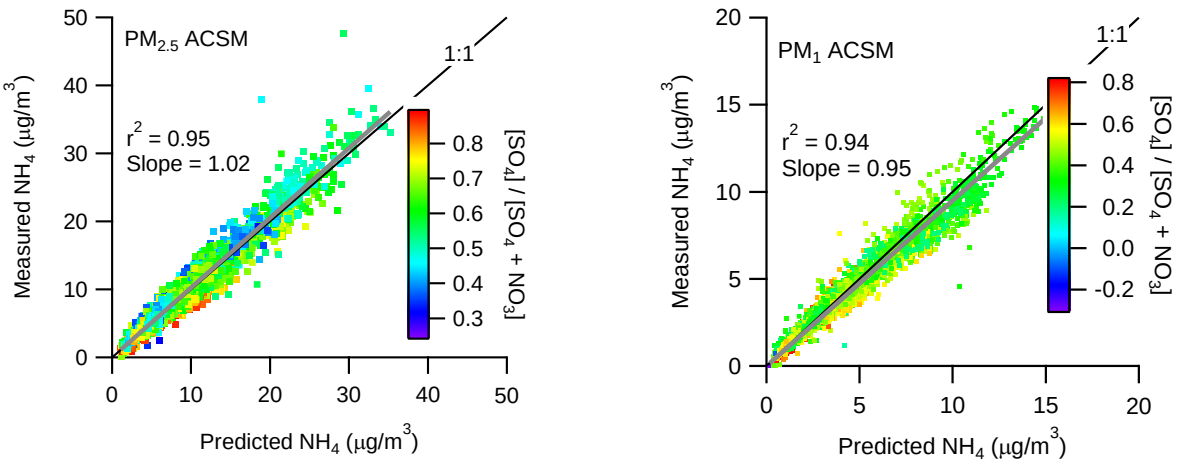

Figure S5. Relationship between measured NH_4 and predicted NH_4 for both the $PM_{2.5}$ and PM_1 ACSMs, respectively. The points in plots are colored by the ratio of $[SO_4]$ / $[SO_4/NO_3]$. Note that predicted NH_4 is estimated by $18 \times (2 \times [SO_4/96] + [NO_3/62] + [Cl/35.5])$.

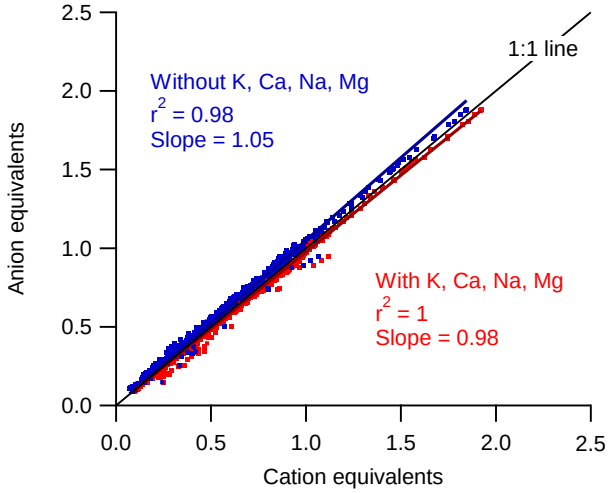

Figure S6. Ion balance of the water-soluble ions measured by the $PM_{2.5}$ MARGA. Note that: anion equivalents = $[NH_4^+/18] + [Na^+/23] + [K^+/39] + [Mg^{2+}/12] + [Ca^{2+}/20]$, and cation equivalents = $[SO_4^{2-}/48] + [NO_3^-/62] + [Cl^-/35.5]$, in which chemical ions are in the unit of $\mu g/m^3$.

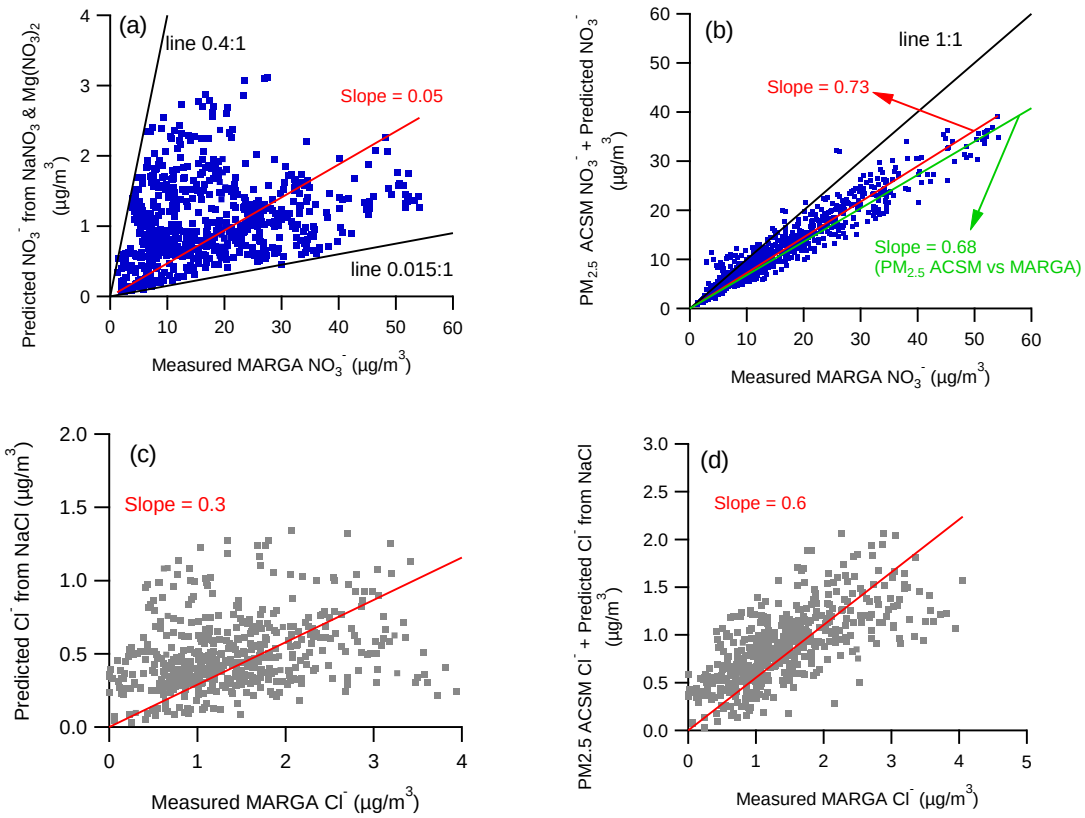

Figure S7. The relationship of (a) predicted NO_3^- (estimated from $NaNO_3$ and $Mg(NO_3)_2$) vs measured MARGA NO_3^-; (b) the sum of predicted NO_3^- and measured $PM_{2.5}$ ACSM NO_3^- vs measured MARGA NO_3^-; (c) predicted Cl^- (estimated from NaCl) vs measured MARGA Cl^-; and (d) the sum of predicted Cl^- and measured $PM_{2.5}$ ACSM Cl^- vs measured MARGA Cl^-.

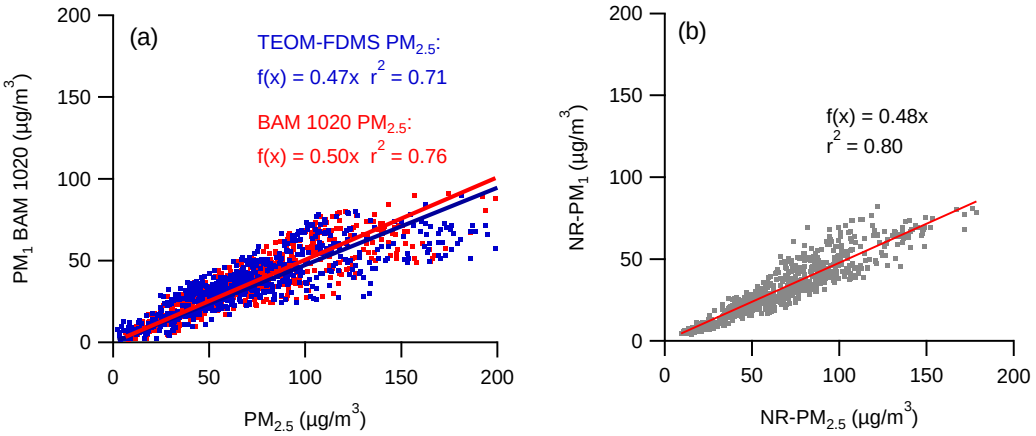

Figure S8. Relationships between (a) PM_1 (measured by Met one BAM1020) and total $PM_{2.5}$ (measured by TEOM-FDMS and Met one BAM1020 respectively) mass loadings; and (b) non-refractory NR-PM_1 (measured by the PM_1 ACSM) and $PM_{2.5}$ (NR-$PM_{2.5}$ measured by the $PM_{2.5}$-ACSM) for the entire study.

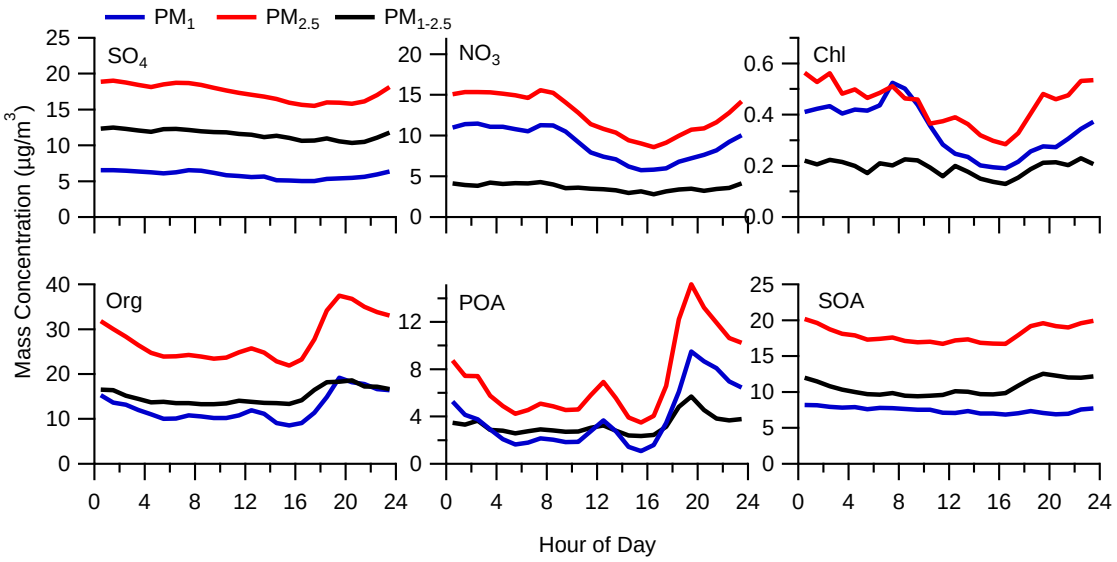

Figure S9. Sized-segregated diurnal variations of fine aerosol species and organic components.

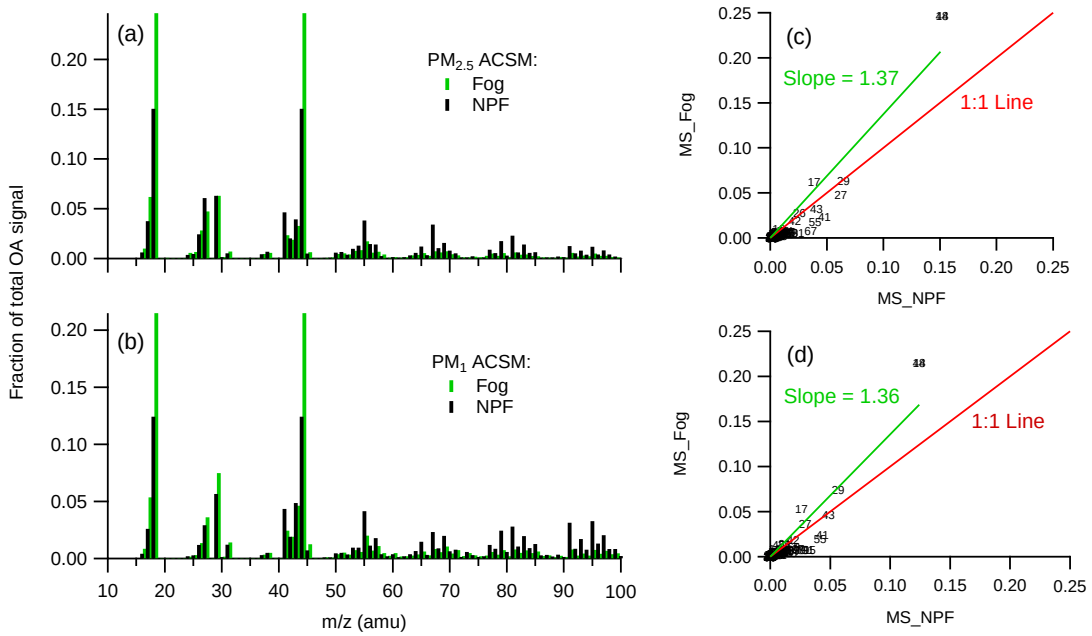

Figure S10. Averaged mass spectra (MS) of OA for PM_1 and $PM_{2.5}$ ACSM during the new particle formation (NPF, Episode 2) and the fog event (Fog, Episode 5) periods, respectively.

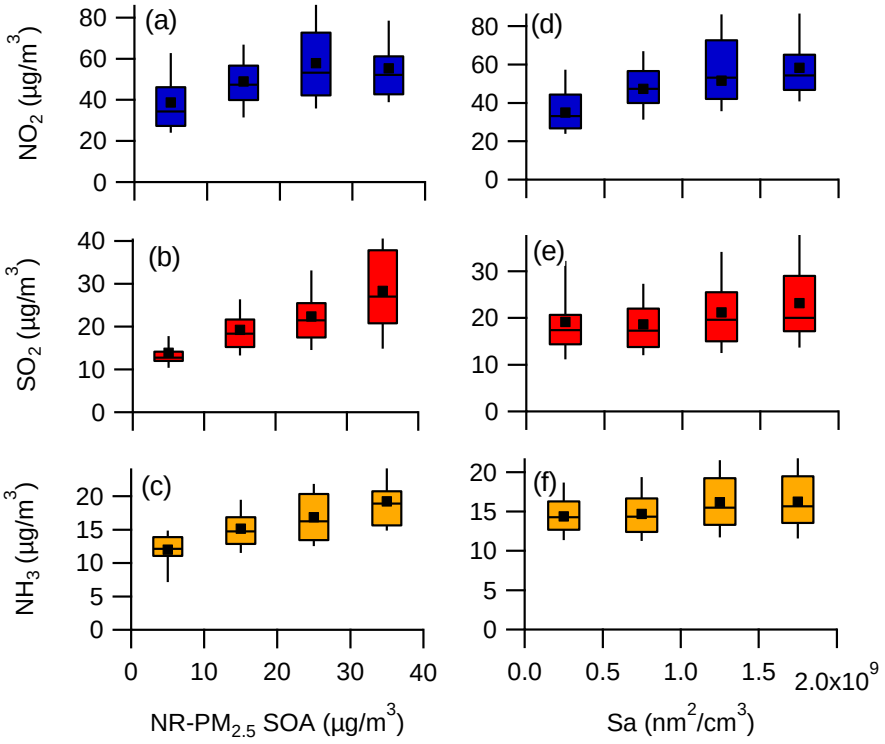

Figure S11. The mass concentrations of NO_2, SO_2, and NH_3 as a function of the NR-$PM_{2.5}$ SOA bins the total particle surface area (S_a) bins, respectively. The median (middle horizontal line), mean (solid squares), 25th and 75th percentiles (lower and upper box), and 10th and 90th percentiles (lower and upper whiskers) are shown for each bin.

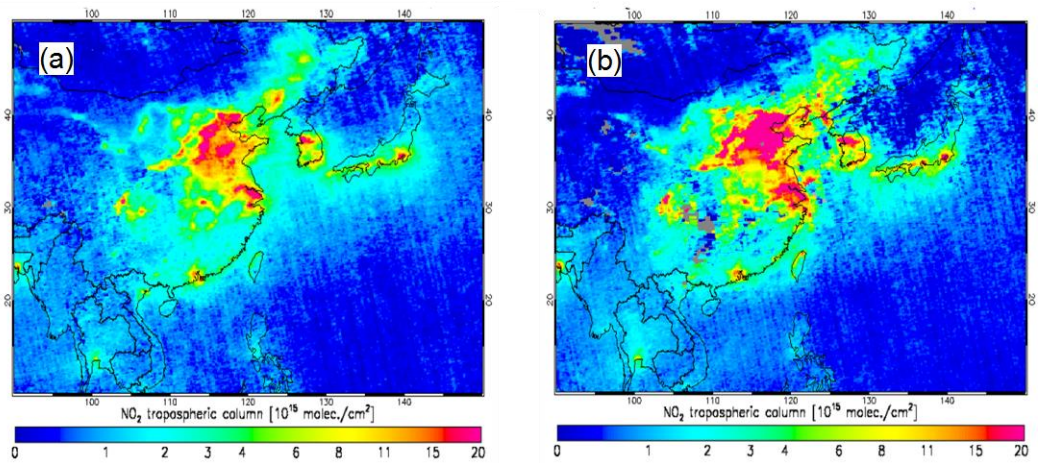

Figure S12. The spatial distribution of monthly mean NO_2 column density (http://www.temis.nl/airpollution/no2.html) in October (a) and November (b) 2015, respectively.

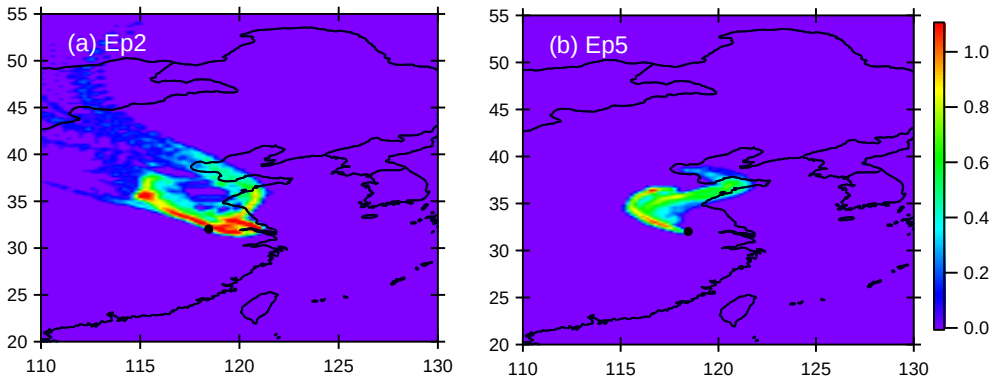

Figure S13. 48 h trajectory arriving at for the new particle formation and growth (a, Episode 2) and foggy (b, Episode 5) events.